

APPLICATION OF BEND STRESS RELAXATION TECHNIQUE TO STUDY OF HIGH TEMPERATURE CREEP OF BULK SILICON CARBIDE CERAMICS—Y. Katoh and L. L. Snead (Oak Ridge National Laboratory)

OBJECTIVE

Bend stress relaxation (BSR) creep experiment was performed using thin strip specimens machined out of chemically vapor deposited (CVD) SiC in two different material classes, in a stress range of general interest for structural ceramics and composites. The primary objective of the experiment was to demonstrate the applicability of BSR technique to the thermal and irradiation creep studies of bulk SiC. Additionally, it was attempted to help understanding the high temperature deformation mechanism for high purity and stoichiometric SiC using the limited data obtained.

SUMMARY

Bend stress relaxation (BSR) creep of two forms of chemically vapor-deposited beta phase silicon carbide, namely polycrystalline and single-crystalline, was studied. The experiment was primarily oriented to demonstrate the applicability of BSR technique to irradiation-induced / enhanced creep behavior of silicon carbide in nuclear environments. It was demonstrated that thin strip samples with sufficient strength for BSR experiment could be machined and the small creep strains occurred in those samples could be measured to sufficient accuracy.

The thermal creep experiment was conducted at 1573–1773K in argon to maximum hold time of 10 hours. Both materials exhibited similar primary creep deformation at the initial stresses of 65–100 MPa. The relative stress relaxation determined in the present experiment appeared significantly smaller than those reported for a commercial CVD SiC fiber at given temperature, implying a significant effect of the initial material conditions on the relaxation behavior. The analysis based on the relaxation time/temperature relationship gave an activation energy of ~ 850 kJ/mol for the primary responsible process in CVD SiC.

PROGRESS AND STATUS

Introduction

Creep property is among the major potential lifetime-limiting factors for high temperature materials, including silicon carbide (SiC) ceramics and SiC-based ceramic composites. SiC-based ceramics and composites are considered for application in advanced fission and fusion power systems [1,2]. In nuclear environments, irradiation-induced/enhanced creep (“irradiation creep”) is added to thermally-activated creep deformation. In many cases, irradiation creep is caused by preferred absorption of supersaturated point defects at edge dislocations in favor of stress relaxation, and hence generally dominates at relatively low temperatures where thermal creep is not of concern [3]. Integrity of gas reactor fuel particles will be affected by creep of SiC shell as the primary fission gas container. Lifetime of SiC-based structural composites in fusion system will be potentially limited by irradiation creep [4].

Irradiation creep data for ceramics are extremely limited because of difficulty in applying conventional pressurized tube technique [5] or other external loading techniques to ceramic samples in nuclear reactors. Bend stress relaxation (BSR), developed for evaluation of creep properties of ceramic fibers [6], is a technique that is easily applicable to irradiation creep studies. BSR technique has been applied to irradiation creep studies on SiC-based ceramics in forms of thin fibers [7]. However, creep properties of bulk SiC (monolithic SiC or matrix material of ceramic composites) might differ significantly from those of SiC-based fibers, because of significant differences in grain size, micro/nano-structures and chemistry. Also, the stress range of concern for bulk SiC is significantly lower than that for fibers in many cases.

In this work, BSR creep experiment was performed using thin strip specimens machined out of chemically vapor deposited (CVD) SiC in two different material classes, in a stress range of general interest for

structural ceramics and composites. The primary objective of the experiment was to demonstrate the applicability of BSR technique to the (irradiation) creep studies of bulk SiC which are not made into a fiber form. Additionally, it was attempted to help understanding the high temperature deformation mechanism for high purity and stoichiometric SiC using the limited data obtained.

Experimental Procedure

Materials

The materials used were CVD-produced polycrystalline and single-crystalline beta-phase SiC. The polycrystalline material was the standard resistivity grade of “CVD-SiC” produced by Rohm and Haas Advanced Materials (Woburn, MA), with manufacturer-claimed purity of > 99.9995%. The crystal grains of CVD-SiC are highly elongated along the growth direction and have a bi-modal size distribution of large (10 ~ 50 μm in column width) and small (typically 1 ~ several μm) grains. The crystal grains are heavily faulted and have a preferred crystallographic orientation of $\langle 111 \rangle$ directions in parallel to the CVD-growth direction but randomly oriented in the normal plane. All the flexural specimens were machined with longitudinal directions normal to the growth direction.

The single-crystalline (referred to as “SC-SiC” hereafter) material was 3C-SiC {100} surface orientation wafer produced by Hoya Advanced Semiconductor Technologies Co., Ltd. (Tokyo, Japan) [8]. The wafer was nitrogen-doped *n*-type with a carrier density of $\sim 1 \times 10^{19} \text{ cm}^{-3}$, and the thickness of 250 μm . The wafer reportedly contains stacking faults with a mean interspacing of $\sim 2\mu\text{m}$ as the dominating defects [9].

The creep specimens were machined into thin strips with dimensions of 25mm x 1mm x 0.05mm. Both faces were polished with 0.06 μm diamond powders in order not to spoil strength. The surfaces of the CVD-SiC strips were normal to the CVD-growth direction. The SC-SiC strips were machined so that the all sides are normal to $\langle 100 \rangle$ orientations.

Fixture and Strain Measurement

Figure 1 shows a schematic illustration of the fixture designed for the SiC creep study. The thin strip specimens are fixed within a narrow gap between curved surfaces of a pair of the loading plates. This configuration was preferred to conventional four-point flexural configuration, in which the specimen temperature may unacceptably deviate from the designated temperature during in-reactor experiments, which relies on volumetric nuclear heating for controlling temperature. Outer dimensions of the assembled fixture were designed to be 40mm x 4mm x 2mm so that it fits into slots for the standard miniature composite tensile specimens in irradiation vehicles. All the fixture parts were made of CVD-SiC to avoid potential chemical reactions.

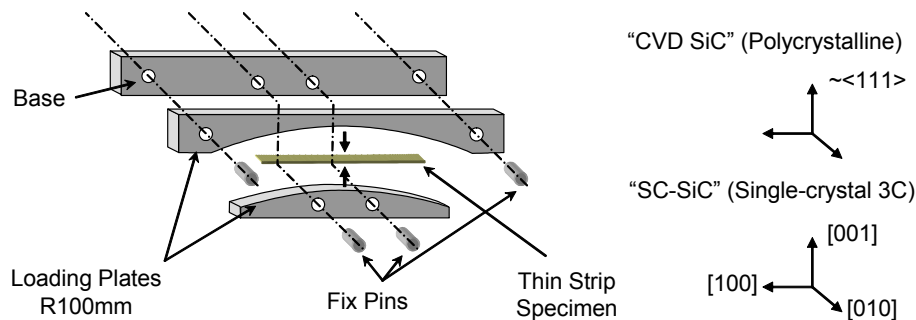


Fig. 1. Illustration of the bend stress relaxation creep fixture designed for in-reactor experiment. All the fixture parts are made of CVD SiC.

Figure 2 shows a photograph of the assembled fixture, and optical micrographs of constrained and relaxed specimens. The bend radius of constrained specimens varied in a range of 120–160mm, depending on gap width in the assembled fixture. Bend radius of the specimens was smallest in the center and largest at the both ends, but the variation was within ~ 10% over the specimen length except for the very end regions. The bend radius averaged over the entire specimen length was used to determine the residual stress after relaxation (σ_a):

$$\sigma_a = \frac{Et(\varphi_0 - \varphi_a)}{2L} \quad (1)$$

where E is the Young's modulus, t the specimen thickness, L the specimen length, φ_0 the initial bend angle, and φ_a the residual bend angle in the freed sample. Thus, the BSR ratio (m) was determined by the equation below:

$$m = \frac{\sigma_a}{\sigma_0} = 1 - \frac{\varphi_a}{\varphi_0} \quad (2)$$

where σ_0 is the initial stresses. The accuracy in bend angle determination by digital optical microscopy was $< 0.1^\circ$. This gives the potential error of ~ 1% in BSR ratio determination regardless of m value in the present experimental configuration.

BSR Conditions

The stress relaxation experiment was performed in a flow of commercial ultra-high purity argon at temperatures of 1573, 1673, and 1773K. The maximum cumulative hold time at the designated temperature was 10 hours. The heating rate at the end of heating sequence was ~ 15K/min. The cooling rate was not controlled but higher than the heating rate. The specimens were measured for creep strain after heat treatment for 1 and 3 hours and then put back to the fixture for further heat treatment. In some occasions, specimens were flipped before additional heat treatment in order to examine the effect of reverse loading. The initial flexural stress levels were estimated to be 65–100 MPa, assuming the room temperature Young's modulus of ~ 450GPa [10] and ~ 94, ~ 93, and ~ 92% retention of the room temperature modulus at 1573, 1673, and 1773K, respectively [11-14].

Results and Discussion

The relaxed bars were curved generally smooth over the length. There was no sign of significantly localized deformation noticed, in a macroscopic scale, in either the relaxed single- and poly-crystalline samples.

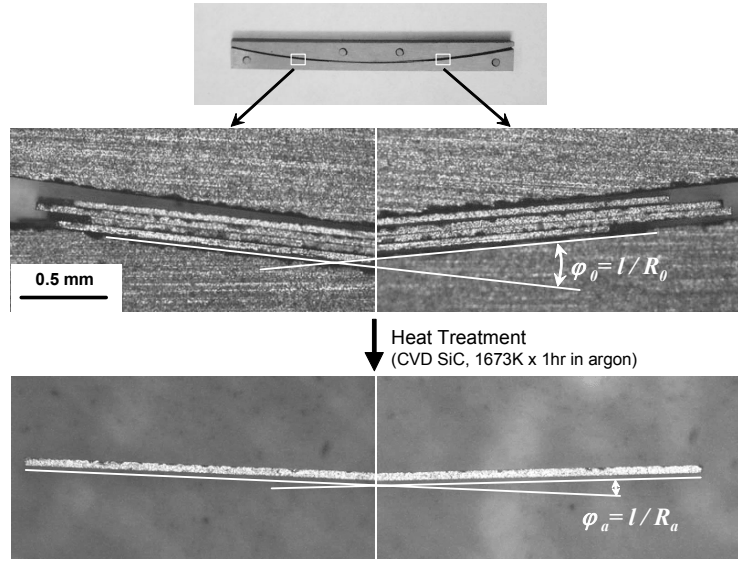


Fig. 2. Measurement of bend radius of constrained and relaxed thin strip samples by optical microscopy.

Flexural stress in the constrained specimens, calculated from the constrained and unconstrained bend radii, is plotted in Fig. 3 as a function of cumulative hold time at the designated temperature. In all cases, the stress exhibited a steep initial drop during the first hour, followed by the periods of much slower relaxation process. Despite of the somewhat varied initial stresses, higher relaxation rates were generally noted at higher temperatures, indicating the responsible mechanism is thermally activated. The residual stress approached to an asymptotic value, which varied but did not appear to systematically depend on materials or temperature. The observed stress relaxation behavior is believed to be due to primary creep, since SiC is known to exhibit only primary creep in the temperature range of this work [15].

CVD-SiC and SC-SiC exhibited similar stress relaxation behavior during the first hour at all temperatures, although the absolute relaxation rate of SC-SiC might be slightly lower than that of CVD-SiC. The residual stress in SC-SiC remained almost unchanged after the first hour of heat treatment, whereas CVD-SiC continued to reduce in stress between 1 and ~ 10 hours. The minimum stresses achieved were higher for SC-SiC than for CVD-SiC at 1673 and 1773K, while they appeared opposite at 1573K, where the initial stress in the CVD-SiC sample was significantly higher than in the SC-SiC sample. Despite of the differences noted above, the similarity in stress relaxation behavior between CVD-SiC and SC-SiC during the first hour suggests that the identical operating mechanism is responsible for the initial stage of the primary creep, eliminating the possibility of major contribution of the grain boundary diffusion and/or sliding [16,17].

Carter et al. reported a lack of compressive stress creep deformation in CVD-SiC at temperatures < 1923K when the specimens were loaded along the CVD-growth direction, and attributed it to the dislocation motion on {111} slip planes as the responsible creep mechanism [18]. If we assume the dislocation glide along <110> directions on {111} planes as the primary operating mechanism, the loading orientation in SC-SiC specimens should give significantly higher average Schmid factor than in CVD-SiC specimens. The possibly lower stress relaxation rate and the higher minimum stress in SC-SiC observed in this work indicate that the operation of such mechanism is unlikely.

Figure 4 plots the BSR ratio, m , against the reciprocal temperature. The m values for CVD-SiC exhibited the expected hold time-dependence, whereas those for SC-SiC did not due to the very small deformation during the period beyond 1 hour. The stress relaxation in the SC-SiC samples needs to be measured after shorter hold time, or preferably be measured by an in-situ type experiment, in order to determine the effect of hold time on the m values.

Assuming a thermally activated relaxation mechanism, the activation energy (Q) for the responsible process can be determined from the temperature dependence of m values at different hold times by the relationship,

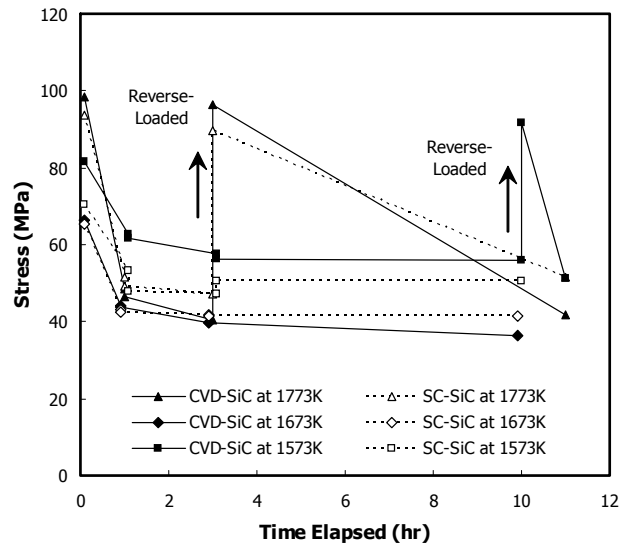


Fig. 3. Relaxation behavior of the maximum surface stress in polycrystal (CVD-SiC) and single-crystal (SC-SiC) beta-SiC samples during BSR experiment. Reverse loading was applied to some specimens by putting back into the fixture after flipping.

$$Q = R \cdot \frac{\ln(t_2/t_1)}{1/T_2 - 1/T_1} \quad (3)$$

where T_1 and T_2 are the temperatures at which m is equal to a constant value after hold times of t_1 and t_2 , respectively [6]. From the present experiment, one can derive the activation energy of ~ 850 kJ/mol. This value is very close to the self diffusion energy of either carbon or silicon in beta-SiC [19-21], implying that the bulk diffusion is a potential controlling mechanism.

However, it should be noted that this analysis may incorporate potentially a large error in estimating the activation energy because of the following reasons. First, the initial stress was not constant but significantly varied in the runs at different temperatures, as seen in Fig. 3. For these materials in the stress range tested, a linear stress dependence of the strain rate has not been demonstrated. Second, the asymptotic values of the remaining stress seem to be dependent on temperature. The asymptotic stress at 1573K and 1673K probably corresponds to $m = \sim 0.5$ in this experiment, so the activation energy would be most accurately determined at the constant value of m at significantly higher than 0.5. However, $m = \sim 0.5$ has already achieved at 1773K after the shortest hold time. Therefore, the optimum m value at which the activation energy could be estimated in a sufficiently credible manner was not identified in the present experiment.

Plotted together in Fig. 4 are the published bend stress relaxation ratio data for SCS-6™ CVD SiC fiber [6], Hi-Nicalon™ Type-S near-stoichiometric polymer-derived SiC fiber [7,22], and a developmental “2 mil” CVD SiC fiber that consists of the core and inner layers for SCS-6 fiber [15]. Data points from the present experiment appear at significantly higher temperatures than those for the CVD SiC fiber for the same m value, implying the smaller extent of stress relaxation in the CVD SiC studied than in the fiber. It is believed that this difference is primarily due to the presence of excess silicon in the outer shell of the SCS-6 CVD SiC fiber. Morscher and DiCarlo have derived an activation energy of ~ 560 kJ/mol for the SCS-6 fiber at $m = 0.5$ and attributed the deformation to anelastic grain boundary sliding controlled by the grain boundary diffusion of excess silicon [6]. On the other hand, m values obtained here are close to those for the Hi-Nicalon™ Type-S fiber, which does not include excess silicon but is slightly rich in carbon. Another potential reason for the different relaxation behavior is the initial strain. In the present experiment, it was $\sim 0.02\%$, while it was $0.1 \sim 0.3\%$ in the referred work by Morscher et al. [6] and Youngblood et al. [7]. The initial stress or strain in the experiment by Sacks is not reported [22].

Specimen reversed in bending direction after experiencing significant stress relaxation exhibited a large initial stress drop similar to that in virgin samples. The residual stress levels reached after heat treatment under the reverse loading were similar to those in non-flipped specimens. These features indicate that the microstructural defect motion responsible for the primary creep deformation is reversible. Further study is necessary to identify the responsible operating mechanism.

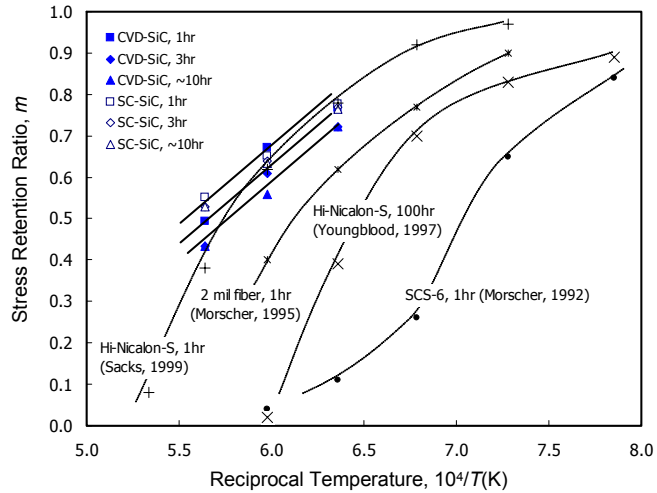


Fig. 4. Bend stress relaxation ratio (m) for in polycrystal (CVD-SiC) and single-crystal (SC-SiC) beta-SiC samples plotted against reciprocal temperature.

References

- [1] R. H. Jones et al., Promise and challenges of SiCf/SiC composites for fusion energy applications, *J. Nucl. Mater.* 307–311 (2002) 1057–72.
- [2] G. O. Hayner et al., Next Generation Nuclear Plant Materials Research and Development Program Plan, INEEL/EXT-04-02347, Revision 1, Idaho National Engineering and Environmental Laboratory, Idaho Falls, Idaho (2004).
- [3] J. L. Straalsund, Radiation Effects in Breeder Reactor Structural Materials, Metallurgical Society of American Institute of Mining, Metallurgical, and Petroleum Engineers, New York (1977).
- [4] R. Scholz and G. E. Youngblood, Irradiation creep of advanced silicon carbide fibers, *J. Nucl. Mater.* 283–287 (2000) 372–75.
- [5] G. W. Lewthwaite, Irradiation creep during void production, *J. Nucl. Mater.* 46 (1973) 324–28.
- [6] G. N. Morscher and J. A. DiCarlo, A simple test for thermomechanical evaluation of ceramic fibers, *J. Am. Ceram. Soc.* 75 (1992) 136–40.
- [7] G. E. Youngblood, R. H. Jones, G. N. Morscher, and A. Kohyama, Creep Behavior for Advanced Polycrystalline SiC Fibers, Fusion Reactor Materials Semiannual Progress Report, DOE/ER-0313/22 (1997) 81–86.
- [8] H. Nagasawa, K. Yagi, and T. Kawahara, 3C-SiC Hetero-epitaxial growth on undulant Si(001) substrate, *J. Crystal Growth* 237–239 (2002) 1244–49.
- [9] E. Polychroniadis, M. Syvajarvi, R. Yakimova, and J. Stoemenos, Microstructural characterization of very thick freestanding 3C-SiC wafers, *J. Crystal Growth* 263 (2004) 68–75.
- [10] Y. Katoh and L. L. Snead, Mechanical Properties of Cubic Silicon Carbide after Neutron Irradiation at Elevated Temperatures, *Journal of ASTM International* (in press).
- [11] J. R. Hellmann, D. J. Green, and M. F. Modest, Physical Property Measurements of High Temperature Composites, in J. R. Hellmann and B. K. Kennedy (eds.), *Projects Within the Center for Advanced Materials* (1990) 95–114.
- [12] W. S. Coblenz, Elastic moduli of boron-doped silicon carbide, *J. Am. Ceram. Soc.* 58 (1975) 530–531.
- [13] R. G. Munro, Material properties of a sintered-SiC, *J. Phys. Chem. Ref. Data* 26 (1997) 1195–1203.
- [14] J. Kubler, Weibull Characterization of Four Hipped/Posthipped Engineering Ceramics Between Room Temperature and 1500°C, *Mechanische Charakterisierung von Hochleistungskeramik Festigkeitsunte*, EMPA Swiss Federal Laboratories for Materials Testing and Research, 1–88 (1992).
- [15] G. N. Morscher, C. A. Lewinsohn, C. E. Bakis, R. E. Tressler, and T. Wagner, Comparison of bend stress relaxation and tensile creep of CVD SiC fibers, *J. Am. Ceram. Soc.* 78 (1995) 3244–52.
- [16] C. A. Lewinsohn, L. A. Giannuzzi, C. E. Bakis, and R. E. Tressler, High-temperature creep and microstructural evolution of chemically vapor-deposited silicon carbide fibers, *J. Am. Ceram. Soc.* 82 (1999) 407–13.
- [17] J. A. DiCarlo, Creep of chemically vapour deposited SiC fibers, *J. Mater. Sci.* 21 (1986) 217–224.
- [18] C. H. Carter, Jr., R. F. Davis, and J. Bentley, Kinetics and mechanisms of high-temperature creep in silicon carbide: II. Chemically vapor deposited, *J. Am. Ceram. Soc.* 67 (1984) 732–40.
- [19] M. H. Hon, R. F. Davis, and D. E. Newbury, *J. Mater. Sci.* 15 (1980) 2073.
- [20] J. Li, L. Porter, and S. Yip, Atomistic modeling of finite-temperature properties of crystalline beta-SiC: II. Thermal conductivity and effects of point defects, *J. Nucl. Mater.* 255 (1998) 139–152.
- [21] F. Gao, W. J. Weber, M. Posselt, and V. Belko, Atomistic study of intrinsic defect migration in 3C-SiC, *Phys. Rev. B* 69 (2004) 245–205.
- [22] M. D. Sacks, Effect of composition and heat treatment conditions on the tensile strength and creep resistance of SiC-based fibers, *J. Eu. Ceram. Soc.* 19 (1999) 2305–15.